THE JOURNAL OF BIOLOGICAL CHEMISTRY VOL. 282, NO. 6, pp. 3904–3917, February 9, 2007
Printed in the U.S.A.

Regulation and Function of Glycogen Synthase Kinase-3 Isoforms in Neuronal Survival*[S]

Received for publication, May 30, 2006, and in revised form, December 1, 2006 Published, JBC Papers in Press, December 5, 2006, DOI 10.1074/jbc.M605178200

Min-Huei Liang and De-Maw Chuang[1]

From the Molecular Neurobiology Section, National Institute of Mental Health, Bethesda, Maryland 20892-1363

Glycogen synthase kinase-3 (GSK-3) is a serine/threonine kinase consisting of two isoforms, α and β. The activities of GSK-3 are regulated negatively by serine phosphorylation but positively by tyrosine phosphorylation. GSK-3 inactivation has been proposed as a mechanism to promote neuronal survival. We used GSK-3 isoform-specific small interfering RNAs, dominant-negative mutants, or pharmacological inhibitors to search for functions of the two GSK-3 isoforms in regulating neuronal survival in cultured cortical neurons in response to glutamate insult or during neuronal maturation/aging. Surprisingly, RNA interference-induced depletion of either isoform was sufficient to block glutamate-induced excitotoxicity, and the resulting neuroprotection was associated with enhanced N-terminal serine phosphorylation in both GSK-3 isoforms. However, GSK-3β depletion was more effective than GSK-3α depletion in suppressing spontaneous neuronal death in extended culture. This phenomenon is likely due to selective and robust inhibition of GSK-3β activation resulting from GSK-3β Ser^{9} dephosphorylation during the course of spontaneous neuronal death. GSK-3α silencing resulted in reduced tyrosine phosphorylation of GSK-3β, suggesting that tyrosine phosphorylation is also a critical autoregulatory event. Interestingly, GSK-3 inhibitors caused a rapid and long-lasting increase in GSK-3α Ser^{21} phosphorylation levels, followed by a delayed increase in GSK-3β Ser^{9} phosphorylation and a decrease in GSK-3α Tyr^{279} and GSK-3β Tyr^{216} phosphorylation, thus implying additional levels of GSK-3 autoregulation. Taken together, our results underscore important similarities and dissimilarities of GSK-3α and GSK-3β in the roles of cell survival as well as their distinct modes of regulation. The development of GSK-3 isoform-specific inhibitors seems to be warranted for treating GSK-3-mediated pathology.

Glycogen synthase kinase-3 (GSK-3)[2] is an evolutionary conserved, ubiquitous serine/threonine kinase that is highly enriched in the brain and consists of two distinct isoforms, α and β, in mammals (1). One of the most notable qualities of GSK-3 is the vast number of signaling pathways that converge on this enzyme and subsequently an even greater number of biological targets (reviewed in Refs. 2–4). To date, numerous studies have indicated that GSK-3 acts as a downstream regulator that determines the outcome of several prominent pathways following stimuli such as Wnt signaling, phosphatidylinositol 3-kinase, and neurotrophic pathways. Dysregulation of GSK-3-mediated substrate phosphorylation and signaling pathways has been implicated in the pathophysiological conditions of a variety of diseases, including Alzheimer disease, type 2 diabetes, and cancer (4); schizophrenia (5); and mood disorders (6). The precise mechanism regulating these distinct pathways upstream and downstream of GSK-3 is not well understood and is an area of active research.

The diverse functions of GSK-3 include regulation of cell activity, structure, and survival (reviewed in Refs. 4 and 7) as well as circadian rhythms (8–10). Such exquisite regulation involves coordinated control of phosphorylation of GSK-3 and its substrates; the formation of substrate-specific GSK-3 binding/scaffolding protein complexes; and GSK-3 subcellular distribution, notably in nuclei and mitochondria (11). It has been suggested that lithium, a direct inhibitor of GSK-3 (12, 13), may exert some of its neuroprotective effects through inhibition of GSK-3 (14–16). In most systems, increased activation of GSK-3β is pro-apoptotic, whereas its inhibition is anti-apoptotic (17–23). A previous study further suggests that inactivation of GSK-3β is a principal regulatory target of the phosphatidylinositol 3-kinase survival pathway (18). However, little information is available as to the effects on neuronal survival resulting from depletion/inhibition of GSK-3α.

The main structural differences between the GSK-3α and GSK-3β isoforms lie in the N- and C-terminal regions, whereas their sequences are highly homologous within the kinase domain. The activities of GSK-3 are positively regulated by phosphorylation of Tyr^{279} and Tyr^{216} for the α- and β-isoforms, respectively, and negatively regulated by N-terminal phosphorylation of Ser^{21} and Ser^{9} for the α- and β-isoforms, respectively (3). GSK-3 is unique in that the kinase is constitutively active in cells under resting conditions and is primarily regulated through inhibition of its activity. In addition, com-

* This work was supported by Intramural Research Program Project Z01MH002468-18 from the National Institute of Mental Health. The costs of publication of this article were defrayed in part by the payment of page charges. This article must therefore be hereby marked "*advertisement*" in accordance with 18 U.S.C. Section 1734 solely to indicate this fact.

[S] The on-line version of this article (available at http://www.jbc.org) contains supplemental "Materials and Methods" and Figs. S1–S3.

[1] To whom correspondence should be addressed: NIMH, Bldg. 10, Rm. 4C-206, 10 Center Dr. MSC 1363, Bethesda, MD 20892-1363. Tel.: 301-496-4915; Fax: 301-480-9290; E-mail: chuang@mail.nih.gov.

[2] The abbreviations used are: GSK-3, glycogen synthase kinase-3; PP1, protein phosphatase-1; siRNAs, small interfering RNAs; DIV, days *in vitro*; MTT, 3-(4,5-dimethylthiazol-2-yl)-2,5-diphenyltetrazolium bromide; AN, annexin V; PI, propidium iodide; FACS, fluorescence-activated cell sorter; PBS, phosphate-buffered saline; AM, acetoxymethyl ester; EthD-1, ethidium homodimer-1; GAPDH, glyceraldehyde-3-phosphate dehydrogenase; CREB, cAMP-responsive element-binding protein; ERK, extracellular signal-regulated kinase; DAPI, 4′,6-diamidino-2-phenylindole; DIC, differential interference contrast; MAPK, mitogen-activated protein kinase.

Supplemental Material can be found at:
http://www.jbc.org/cgi/content/full/M605178200/DC1

pared with other protein kinases, GSK-3 has its preference for primed substrates, *i.e.* substrates previously phosphorylated by another kinase (4). The phosphorylation state of serine residues of both isoforms is dynamic, involving phosphorylation mainly by diverse kinases (4) and dephosphorylation by protein phosphatase-1 (PP1) (24). Autophosphorylation of both serine and tyrosine residues in GSK-3 has been reported and suggests that GSK-3 regulates its own phosphorylation status (24–26). Although some evidence supports active regulation of tyrosine phosphorylation in the brain (21), the vast majority of research on GSK-3 has been focused on the aspect of inhibitory serine phosphorylation, and little is known about possible kinases involved in GSK-3 activation through tyrosine phosphorylation. In addition, previous studies have led to conflicting conclusions as to whether the tyrosine phosphorylation of GSK-3 is catalyzed by GSK-3 itself or by a distinct tyrosine kinase (25–30).

Despite their similar biochemical and substrate properties, GSK-3α and GSK-3β are not always functionally identical (31–35). In addition, differential expression of GSK-3α and GSK-3β in different tissues (1) and their subcellular localizations (36–39) have also been demonstrated. Dynamic regulation of GSK-3 kinase activity through modulation of serine/tyrosine phosphorylation in neurons at different developmental/maturation stages is thus possibly mediated via diverse spatial/temporal distribution of these two GSK-3 isoforms. Accordingly, a better understanding of the state of GSK-3 serine/tyrosine phosphorylation of each isoform in response to stimulation is necessary to address these critical issues.

In this study, we used pharmacological inhibitors, GSK-3 isoform-specific small interfering RNAs (siRNAs), wild-type GSK-3α and GSK-3-β, and their dominant-negative mutants to address their differential functions and regulation in cultured rat cerebral cortical neurons. We first investigated the role of GSK-3 isoforms in the execution of and protection against glutamate-induced excitotoxicity. We then assessed their states of serine and tyrosine phosphorylation and neuronal survival following GSK-3 inhibition as well as during various stages of neuronal cultures to explore their functional involvements.

MATERIALS AND METHODS

Rat Primary Cerebral Cortical Culture—Preparation of cerebral cortical neurons from 18-day-old embryonic rats was performed as described previously (40) with modifications (41). Cortical neurons were used for transfection after 9 days *in vitro* (DIV) unless indicated otherwise.

siRNA Preparation—Several rat-specific siRNAs targeting either isoform of GSK-3 were as described previously (41). They are αP747, αP1269, αP1375, βP555, βP514, βP1093, and $\alpha\beta$P1357. siRNA $\alpha\beta$P1357 is the only siRNA that targets both GSK-3 isoforms. The siRNA mixture specific to either GSK-3 isoform consists of the three species of isoform-specific siRNAs described above. Unless indicated otherwise, GSK-3 siRNA mixtures were used in all silencing experiments. A control siRNA (control non-targeting siRNA-1, Dharmacon, Chicago, IL) was used as an RNA interference control for all siRNA transfection experiments.

Plasmid DNA—Wild-type GSK-3α and its dominant-negative mutant (pMT2/hGSK3α and pMT2-KRhGSK3α, respectively) and the construction of wild-type GSK-3β and two GSK-3β dominant-negative mutants (pEGFP-GSK3β-wt, pEGFP-GSK3β-K85R, and pEGFP-GSK3β-R96A, respectively) were as described previously (41).

Transfection Assays—To determine whether the siRNA was efficiently delivered to the cytoplasm of cortical neurons, we labeled siRNA duplexes with Cy3 using the Silencer™ siRNA labeling kit (Ambion, Inc., Austin, TX) prior to transfection. The siRNA transfection condition was optimized using siPORT *Amine* transfection reagent (Ambion, Inc.) for cortical neurons. Rat primary cortical cultures were evenly plated and cultured for 9 DIV before transfection for 48 h with 80 nM siRNA using 8 μl of siPORT *Amine* in 1 ml of the transfection mixture. Transfection of GSK-3 expression vectors (wild-type or dominant-negative mutants) into primary cortical neurons were established using a Nucleofector device (Amaxa GmbH, Cologne, Germany) in conjunction with a rat neuron Nucleofector kit (Amaxa GmbH) at the time of cell plating as described (41).

GSK-3 Inhibitors—Two structurally unrelated non-ATP-competitive GSK-3β inhibitors, inhibitor I (TDZD-8, thiadiazolidinone analog) and inhibitor VII (α-4-dibromoacetophenone), were purchased from Calbiochem. Two structurally similar ATP-competitive GSK-3 inhibitors, SB 216763 and SB 415286, were purchased from Tocris Bioscience (Ellisville, MO). Lithium salt (LiCl) was obtained from Sigma.

Cell Viability Analysis—Cell viability was determined by the 3-(4,5-dimethylthiazol-2-yl)-2,5-diphenyltetrazolium bromide (MTT) assay as described (40). Annexin V (AN)-propidium iodide (PI) double staining and fluorescence-activated cell sorter (FACS) analysis were also performed to detect pre-apoptotic and dead cells, respectively. Briefly, cells were harvested using trypsin/EDTA solution, washed once with ice-cold phosphate-buffered saline (PBS), and double-stained with 5 μl of Alexa Fluor 488-conjugated AN (Molecular Probes, Eugene, OR) to detect externalized phosphatidylserine during apoptosis and 1.5 μM PI (Sigma) in 100 μl of annexin V binding buffer (10 mM HEPES, 140 mM NaCl, and 2.5 mM $CaCl_2$ (pH 7.4)) according to the manufacturer's recommendations. Additionally, cell viability was determined by lactate dehydrogenase cytotoxicity detection assay and calcein acetoxymethyl ester (AM)/ethidium homodimer-1 (EthD-1) live/dead cell detection assay. Briefly, 96-well cultures (2000 cells/well) were transfected with GSK-3 isoform-specific siRNA or non-targeting control siRNA by electroporation using a Nucleofector device in conjunction with a rat neuron Nucleofector kit formulated for primary rat cortical neurons at the time of cell plating. Cells were harvested at the indicated DIV, and cell viability was performed using a lactate dehydrogenase cytotoxicity detection kit (Roche Diagnostics GmbH, Penzberg, Germany) according to the manufacturer's recommendations. Similarly, at the indicated DIV, cells were incubated with 3 μM calcein-AM and 1 μM EthD-1 (live/dead viability/cytotoxicity kit, Molecular Probes) at room temperature for 45 min to simultaneously detect live and dead cells, respectively. This procedure produced two-color fluorescence to determine live and dead cells, which were quantified with a fluorescence microplate reader using the appropriate filters

(Wallac 1420 multilabel counter, PerkinElmer Life Sciences, Turku, Finland) and WorkOut Applications data management software (PerkinElmer Life Sciences). Additionally, at the indicated DIV, cultured cortical cells plated on poly-D-lysine-coated chambered coverglasses (Lab-Tek II No. 1.5 borosilicate coverglass, Nalge Nunc International, Rochester, NY) were incubated with 6 μM calcein-AM and 2 μM EthD-1 (live/dead viability/cytotoxicity kit) in Dulbecco's PBS (Invitrogen) at room temperature for 45 min. Following incubation, cells were washed once with Dulbecco's PBS, and images of green fluorescence (calcein-AM)-labeled live cells and red fluorescence (EthD-1)-labeled dead cells were examined by laser scanning confocal microscopy (Zeiss LSM 510 413, Carl Zeiss AG, Oberkochen, Germany). Z-sectioning images were captured with a Zeiss digital camera and analyzed using Zeiss LSM 5 software (Version 3.2).

FACS Analysis—Cy3-labeled siRNA targeting GSK-3α or GSK-3β was transfected into rat cortical neurons at 9 DIV. Forty-eight h after transfection, $\sim 3 \times 10^6$ cortical cells were trypsinized, resuspended in 0.5 ml of PBS, and fixed overnight in 5 ml of 70% ethanol at 4 °C. The cells were then washed twice with ice-cold PBS containing 0.5% bovine serum albumin. The transfection efficiency was determined by FACS analysis (EPICS XL-MCL flow cytometer, Beckman Coulter, Fullerton, CA). Data curves were fitted using the ModFit LT software package (Verity Software House, Topsham, ME). In a separate viability assay experiment, AN-PI double staining and FACS analysis were performed to detect pre-apoptotic cells. Flow cytometry was performed to detect PI (red) and AN (fluorescein isothiocyanate; green) staining of dead and pre-apoptotic cells, respectively. The cellular DNA content and AN labeling were determined by FACS analysis. Data curves were fitted using the WinList software program (Verity Software House).

Immunoblot Analysis—Cortical neurons were washed twice with 5 ml of PBS and harvested by scraping into cell lysis buffer (Cell Signaling Technology, Beverly, MA) supplemented with protease inhibitor mixture (Roche Diagnostics GmbH, Basel, Switzerland). Protein concentrations were determined using a BCA protein assay reagent kit (Pierce). Typically, an aliquot of 20 μg of protein was loaded onto each well of a 4–12% SDS-polyacrylamide gel and separated by electrophoresis. The proteins were then transferred to a nitrocellulose membrane, which was further incubated with the indicated antibodies using standard protocols. Antibodies against GSK-3α, GSK-3β, β-actin, β-catenin, and CDK5 (cyclin-dependent kinase-5) were purchased from Santa Cruz Biotechnology, Inc. (Santa Cruz, CA). Antibody against glyceraldehyde-3-phosphate dehydrogenase (GAPDH) was obtained from Upstate (Charlottesville, VA). Antibodies against phospho-GSK-3α Ser^{21}, phospho-GSK-3β Ser^{9}, phospho-GSK-3$\alpha\beta$ Tyr$^{279/216}$, phospho-cAMP-responsive element-binding protein (CREB) Ser^{133}, phospho-ERK (p44/42), phospho-AKT Ser^{476}, CREB, ERK, and AKT were products of Cell Signaling Technology. An ECL Plus Western blotting detection system (Amersham Biosciences, Little Chalfont, UK) was used to obtain Western blot signals, and autoradiographs were scanned. The intensity of immunoblot signals was analyzed using Scion Image for Windows (Scion Corp.).

Immunocytochemistry—Poly-D-lysine-coated chambered coverglasses (Lab-Tek II No. 1.5 or 1.0 borosilicate coverglass) were used for cortical neuronal cultures. Cortical neurons at 9 DIV were transfected with siRNAs for GSK-3α and GSK-3β as described above. Forty-eight h after transfection, cells were washed with ice-cold PBS and then fixed in phosphate-buffered 4% paraformaldehyde (FD NeuroTechnologies, Baltimore, MD) for 15 min at room temperature. Following fixation, cells were washed three times with ice-cold PBS and then incubated with 300 nM 4′,6-diamidino-2-phenylindole (DAPI; Molecular Probes) in PBS for 10 min. For the detection of Cy3-labeled siRNAs and DAPI-stained nuclei, cortical cells were visualized by laser scanning confocal microscopy (Zeiss LSM 510) with the appropriate filters, and Z-sectioning images were captured using a digital camera and software as described above. To assess co-localization of Cy3 siRNAs and DAPI-stained nuclei, we used a Zeiss ApoTome device for Z-sectioning. For the detection of phospho-GSK-3β Ser^{9}, anti-phospho-GSK-3β Ser^{9} antibody (1:500 dilution) and fluorescein isothiocyanate-conjugated IgG (1:500 dilution; Santa Cruz Biotechnology, Inc.) were used. The coverglasses were mounted using VECTASHIELD mounting medium with DAPI (H-1200, Vector Laboratories, Burlingame, CA) and viewed by confocal fluorescence microscopy as described above. For the detection of pre-apoptotic cells, the AN conjugate was used with a slight modification of the manufacturer's protocol. Briefly, cortical neurons at 12 DIV were washed with cold PBS, followed by incubation in annexin binding buffer. Cells were then double-stained with 25 μl of AN conjugate and 0.8 μM PI in 100 μl of reaction mixture for 25 min at room temperature, followed by washing three times with annexin binding buffer. The coverglasses were then viewed by confocal microscopy (Zeiss LSM 510), and images were captured as described above.

Statistical Analysis—Results are presented as the means ± S.E. from three independent experiments. The results were analyzed for statistical significance by GraphPad InStat (GraphPad Software, San Diego, CA) by Student's *t* test or one-way analysis of variance. In analysis of variance, a quantile-quantile plot was adopted for normal distribution tests, and Turkey's post hoc test was adopted if the variances between groups were similar.

RESULTS

Selective Silencing and Neuroprotective Effects Induced by siRNA for GSK-3α or GSK-3β in Rat Cortical Neurons—We first established high efficiency transfection of siRNA into rat cerebral cortical neurons using the siPORT *Amine* transfection reagent. Rat cortical neurons at 9 DIV were transfected with various concentrations (20–80 nM) of siRNA targeted specifically against GSK-3β. Confocal imaging results using 60 nM Cy3-labeled siRNA showed uptake of GSK-3β-targeted siRNAs into cortical neurons 48 h after transfection (Fig. 1*A*). The *arrows* in the merged image indicate examples of cultured cortical neurons with co-localized Cy3-labeled siRNAs and DAPI-stained nuclei. FACS dot plots of Cy3-positive cells showed the dose-dependent, highly effective transfection of GSK-3β siRNA, with ~80% of cells being transfected at 80 nM (Fig. 1, *B–G*). Similar transfection efficiency was achieved when siRNA

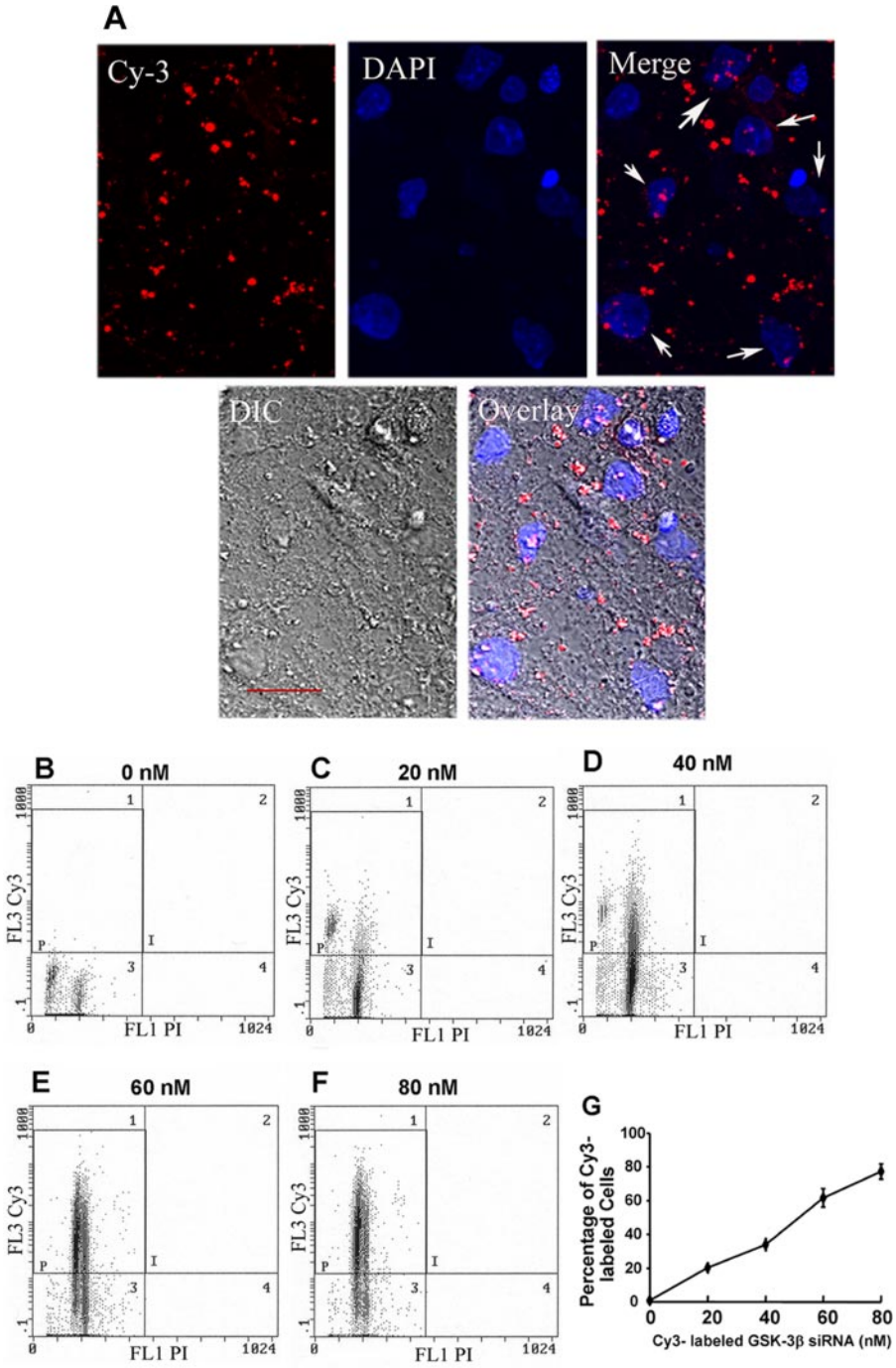

FIGURE 1. **High efficiency transfection of Cy3-labeled GSK-3β siRNA into rat cortical neurons.** *A*, confocal images of double immunofluorescence of cortical neurons at 11 DIV with Cy3-labeled GSK-3β siRNAs (Cy3; *red*) and DAPI (*blue*). The merged image shows the localization of Cy3-labeled siRNAs and DAPI-stained nuclei. The *arrows* indicate neurons successfully transfected with Cy3-labeled GSK-3β siRNAs. The overlay image shows localization of neurons with Cy3-DAPI double immunofluorescence overlaid on a Nomarski-DIC image. Sixty nM GSK-3β (βP555) siRNA was labeled with Cy3 using an siRNA labeling kit and transfected into cortical neurons using siPORT *Amine* transfection reagent. Z-sectioning confocal images were obtained by Zeiss LSM 510 microscopy using a digital camera 48 h after transfection with siRNAs. Representative images are shown. *Scale bar* = 20 μm. *B–F*, detection of Cy3-labeled GSK-3β siRNA was assayed by FACS analysis 48 h after transfection at the indicated concentrations: 0 nM (reagent control; *B*), 20 nM (*C*), 40 nM (*D*), 60 nM (*E*), and 80 nM (*F*). *G*, quantification of the percentage of cortical neurons transfected with Cy3-labeled siRNAs. The quantified data are expressed as the means ± S.E. of cell counts from three independent cultures.

for GSK-3α was employed (data not shown). These results were confirmed by a comparable experiment using manual counting of cells on slides, which produced results similar to those obtained by flow cytometry (data not shown).

Western blotting was performed to assess the silencing effects of siRNA for GSK-3α or GSK-3β. Transfection of cortical neurons with 80 nM siRNA mixtures for either GSK-3α or GSK-3β alone or a combination of siRNAs targeting both GSK-3α and GSK-3β resulted in 70–80% knockdown of their respective proteins 48 h after transfection, whereas the protein levels of the non-targeted GSK-3 isoforms were unaffected (Fig. 2, *A* and *B*). A commercially available antibody that recognizes both GSK-3 isoforms was used to examine the abundance of both GSK-3 isoforms in cortical neurons. GSK-3β was found to be predominant, and GSK-3α accounted for only 35% of the total GSK-3 protein in cortical neurons treated with non-targeting siRNA (Fig. 2*A*).

We then examined the significance of GSK-3 isoform gene silencing with respect to neuronal survival. Surprisingly, pretreatment of cortical neurons with siRNA for either GSK-3α or GSK-3β was sufficient to protect neurons against excitotoxicity resulting from 24-h glutamate exposure (Fig. 2*C*). Similar neuroprotective effects were observed when cortical neurons were transfected with siRNA for GSK-3$\alpha\beta$ (which knocked down both α- and β-isoforms of GSK-3) (Fig. 2*C*) or pretreated with GSK-3 inhibitors, including lithium chloride, the ATP-competitive inhibitors SB 216763 and SB 415286, and the ATP-non-competitive inhibitor I and inhibitor VII (Fig. 2, *C* and *D*). Similarly, inhibition of GSK-3 kinase activity by transfection with dominant-negative forms of either GSK-3α or GSK-3β partially protected cortical neurons from glutamate-induced excitotoxicity (Fig. 2*E*). In contrast, overexpression of wild-type GSK-3α or GSK-3β induced neurotoxicity in the absence of glutamate and potentiated the toxicity in the presence of glutamate. These results suggest a critical role for both GSK-3α and GSK-3β in mediating glutamateinduced excitotoxicity, which has been previously shown to be mediated by *N*-methyl D-aspartate receptors (40).

Experiments were also carried out to detect pre-apoptotic neurons induced by glutamate treatment. Glutamate-treated

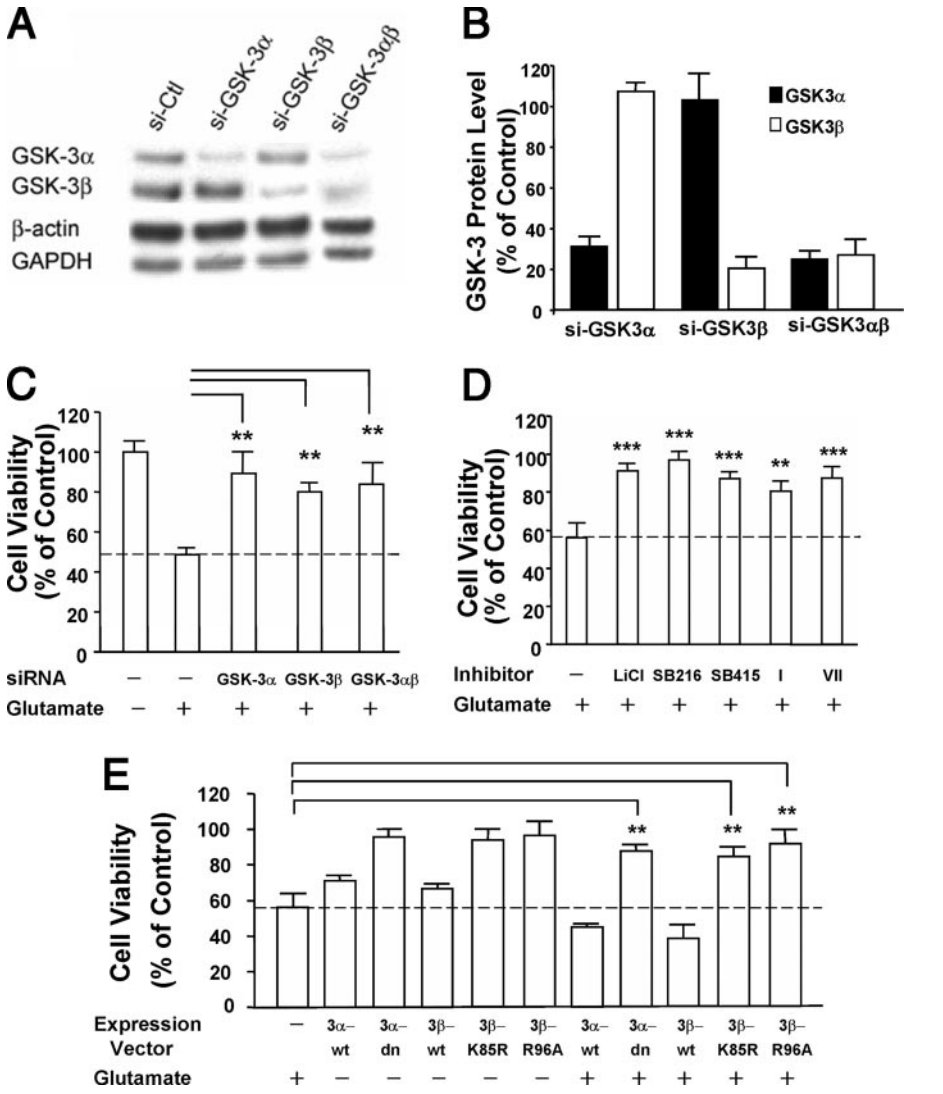

FIGURE 2. **siRNA-mediated silencing of GSK-3α and/or GSK-3β and GSK-3 inhibition protect against glutamate-induced excitotoxicity in cortical neurons.** *A*, Western blot demonstrating selective reduction in GSK-3α and GSK-3β protein levels after treatment with GSK-3 isoform-specific siRNA (*si-GSK-3*) mixtures for 48 h, starting at 9 DIV. β-Actin and GAPDH were used as loading controls. *si-Ctl*, non-targeting control siRNA. *B*, quantification of the percentage reduction in GSK-3 isoform protein after treatment with a GSK-3 isoform-specific siRNA mixture. The results are expressed as the means ± S.E. of the percentage of protein levels with non-targeting control siRNA from three independent cultures. *C*, neuroprotective effects induced by selective depletion of GSK-3α and/or GSK-3β. Cortical neurons were transfected with 80 nM GSK-3 isoform-specific siRNAs at 9 DIV, followed by treatment with 40 μM glutamate at 11 DIV for 24 h. Cell viability was measured by MTT assay at 12 DIV. **, $p < 0.01$ compared with the respective glutamate-treated control. *D*, neuroprotective effects of GSK-3 inhibitors. Cortical cultures were pretreated with 1 mM LiCl, 3 μM SB 216763 (*SB216*), 10 μM SB 415286 (*SB415*), 5 μM inhibitor I, or 1 μM inhibitor VII for 48 h starting at 9 DIV and then treated with 40 μM glutamate for 24 h. Cell viability was measured by MTT assay at 12 DIV. **, $p < 0.01$ compared with the glutamate-treated control; ***, $p < 0.001$. *E*, neuroprotective effects of overexpression of GSK-3 dominant-negative mutants. At the time of plating, cortical neurons were transfected with 4 μg of GSK-3 expression vector, wild-type GSK-3α (*3α-wt*) or GSK-3β (*3β-wt*), or mutant GSK-3 (dominant-negative GSK-3α (*3α-dn*), GSK-3β(K85R) (*3β-K85R*), or GSK-3β(R96A) (*3β-R96A*)) using a Nucleofector device. Cultures were continued for 11 days, followed by 40 μM glutamate treatment at 11 DIV for 24 h. Cell viability was measured by MTT assay at 12 DIV. **, $p < 0.01$ compared with the respective glutamate-treated control. The results in *C–E* are expressed as the means ± S.E. of relative cell viability from three independent cultures.

cortical neurons were double-stained with Alexa Fluor 488-conjugated AN and PI to label pre-apoptotic and dead cells, respectively (Fig. 3*A*). Confocal images were captured, and two populations of neurons were identified as AN^+/PI^- pre-apoptotic cells and AN^+/PI^+ dead cells (Fig. 3*A*). Nomarski-differential interference contrast (DIC) imaging showed glutamate-induced damage characterized by loss of neurites (Fig. 3*A*, *lower left panel*). The AN^+/PI^- pre-apoptotic cells, which showed externalized phosphatidylserine on cell surfaces but still maintained membrane integrity (Fig. 3*A*), represented ~30% of the population measured by FACS analysis 24 h after glutamate exposure, whereas the total number of dead cells detected by PI staining was ~45% (Fig. 3*B*). Our results demonstrate that single gene silencing of either GSK-3α or GSK-3β almost completely prevented the appearance of both types of cells. These data are consistent with the results of previous studies documenting that inhibition of GSK-3β contributes to cell survival, whereas hyperactivation of GSK-3β promotes cell death (18, 20–22, 42). Moreover, our results further suggest that GSK-3α inhibition is also critically involved in neuroprotection.

GSK-3 Gene Silencing and Inhibition Cause Increased Serine Phosphorylation, Decreased Tyrosine Phosphorylation, and Increased β-Catenin Protein Levels—As shown above, protein depletion of either GSK-3 isoform was sufficient to protect cortical neurons against glutamate-induced excitotoxicity. Moreover, the neurotoxic effects of glutamate were nearly completely blocked by silencing the minor isoform, GSK-3α, despite the presence of the remaining GSK-3. It has been reported that lithium treatment enhances the Ser^{21} phosphorylation of GSK-3α in cerebellar granule cells (43) and that increased N-terminal serine phosphorylation by inhibition of GSK-3β could promote neuronal survival (14–16). Furthermore, reduced expression or activity of GSK-3 was found to increase its N-terminal phosphorylation in Chinese hamster ovary cells (24). Thus, we examined the states of serine/tyrosine phosphorylation and autoregulation of GSK-3 after isoform-specific protein depletion in an attempt to shed light on GSK-3 siRNA-elicited neuroprotection. When the levels of GSK-3α protein were reduced by transfection of cortical neurons with three siRNAs (αP1375, αP1269, and αP747), the levels of normalized GSK-3β Ser^9 phosphorylation increased, with little change in total GSK-3β protein levels as measured by Western blot analysis

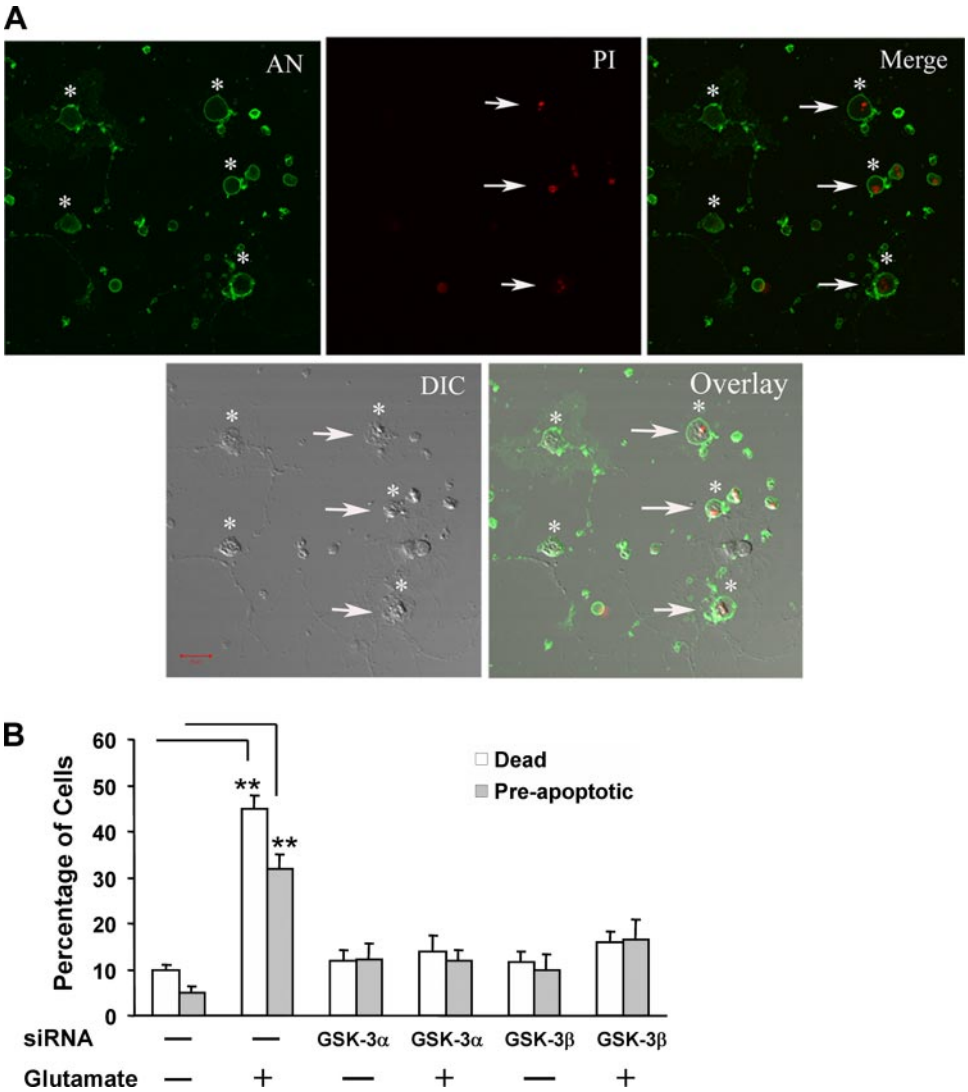

FIGURE 3. **Neuroprotective effects of GSK-3α and GSK-3β siRNAs against glutamate excitotoxicity as assessed by FACS analysis.** Rat cortical neurons were transfected with GSK-3 siRNAs and treated with 40 μM glutamate as described in the legend to Fig. 2 and then subjected to FACS analysis. Alexa Fluor 488-conjugated AN (*green*) and PI (1.5 μM; *red*) were used for staining pre-apoptotic and dead cells, respectively. *A*, Alexa Fluor 488-conjugated AN staining of externalized phosphatidylserine on the surface of cells undergoing apoptosis. Confocal images were captured by Zeiss LSM 510 microscopy using a digital camera. The PI-stained image and merged image are shown for comparison. Examples of AN^+/PI^- pre-apoptotic cells and AN^+/PI^+ dead cells are marked by *asterisks* and *arrows*, respectively. The overlay image shows localization of neurons with AN-PI double immunofluorescence overlaid on a Nomarski-DIC image. Representative images are shown. *Scale bar* = 20 μm. *B*, silencing of GSK-3α or GSK-3β blocks glutamate-induced increases in pre-apoptotic and dead cells. GSK-3 siRNA treatment robustly reduced AN^+/PI^- pre-apoptotic and AN^+/PI^+ dead cells. The results represent the means ± S.E. of the percentage of dead and apoptotic cells in the total population from four independent cultures. **, $p < 0.01$.

(Fig. 4, *A*–*C*). Moreover, a robust increase in the relative GSK-3α Ser^{21} phosphorylation levels normalized to the remaining GSK-3α protein was also observed (Fig. 4*C*). Similar increases in the levels of GSK-3 isoform N-terminal phosphorylation were found when three siRNAs for GSK-3β and one siRNA for both GSK-3α and GSK-3β were individually employed to silence the expression of the GSK-3 isoform (Fig. 4, *A*–*C*).

Immunocytochemical staining and confocal/Z-sectioning imaging of phospho-GSK-3β Ser^9 further confirmed that treatment of cortical neurons with GSK-3α-specific siRNA enhanced GSK-3β Ser^9 phosphorylation and, intriguingly, the nuclear translocation of phospho-GSK-3β Ser^9 compared with the cultures treated with non-targeting control siRNA (Fig. 4*E*). Double fluorescence labeling in the merged images demonstrated a striking co-localization of phospho-GSK-3β Ser^9 and DAPI-stained nuclei in cortical neurons transfected with siRNAs targeting GSK-3α, whereas neurons transfected with non-targeting control siRNA showed cytoplasmic staining of phospho-GSK-3β Ser^9 (Fig. 4*E*). In contrast, transfection with siRNAs for GSK-3α or GSK-3$\alpha\beta$ increased the relative levels of GSK-3α Tyr^{279} phosphorylation, but GSK-3α-specific siRNA distinctly decreased those of GSK-3β Tyr^{216} phosphorylation (Fig. 4*D*). However, siRNAs for GSK-3β slightly decreased tyrosine phosphorylation of both GSK-3α and GSK-3β. These results suggest that the serine and tyrosine phosphorylation levels of GSK-3 isoforms are distinctly regulated in response to GSK-3 depletion.

It is known that β-catenin acts as a downstream transcriptional activator of Wnt signaling by accumulating in the nucleus and forming a complex with DNA-binding proteins such as lymphoid enhancer factor-1 and T-cell factor to regulate T-cell factor-dependent transactivation (reviewed in Ref. 3). In addition, phosphorylation of β-catenin by GSK-3β results in rapid degradation of β-catenin in the cytoplasm (3). Therefore, the inhibition of GSK-3 activity results in the accumulation of β-catenin. We found that enhanced serine phosphorylation of both isoforms was accompanied by accumulation of β-catenin protein in cortical neurons transfected with various GSK-3 siRNAs (Fig. 4, *A* and *B*), further demonstrating inhibition of GSK-3 activity regardless of the state of tyrosine phosphorylation. Inhibition of GSK-3 activity is also supported by our previous observation that cortical neurons transfected with either of the GSK-3 isoform-specific siRNAs and T-cell factor/lymphoid enhancer factor-luciferase reporter show increased activation of T-cell factor/lymphoid enhancer factor transcriptional activity (41).

The increased levels of $Ser^{21/9}$ phosphorylation of GSK-3α/β and the decreased levels of GSK-3β tyrosine phosphorylation caused by single GSK-3 gene silencing suggest a decrease in

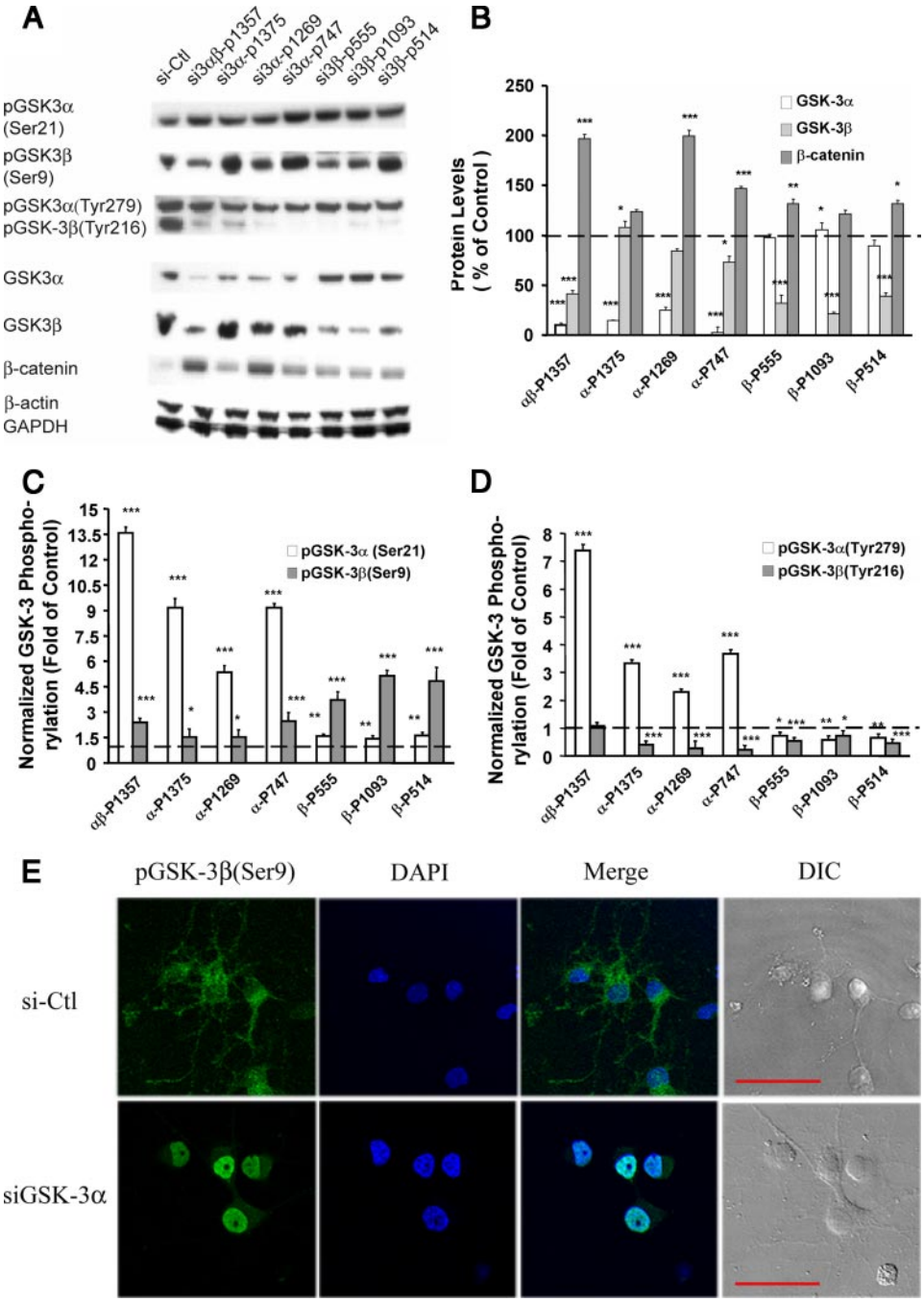

FIGURE 4. **Autoregulation of phospho-GSK-3α Ser^{21}/phospho-GSK-3β Ser^{9} and phospho-GSK-3α Tyr^{279}/phospho-GSK-3β Tyr^{216} induced by GSK-3 isoform-specific siRNAs.** Instead of the siRNA mixture, each siRNA specific for a GSK-3 isoform target sequence was used in transfection. *A*, representative Western blot analysis of the levels of phospho-GSK-3α Ser^{21}, phospho-GSK-3β Ser^{9}, phospho-GSK-3α Tyr^{279}, phospho-GSK-3β Tyr^{216}, GSK-3α, GSK-3β, and β-catenin 48 h after siRNA transfection. β-Actin and GAPDH were used as loading controls. *pGSK3*, phospho-GSK-3; *si-Ctl*, non-targeting control siRNA; *si3*, GSK-3 siRNA. *B*, quantitative results showing changes in the protein levels of GSK-3α, GSK-3β, and β-catenin after isoform-specific siRNA treatment. *C*, quantitative results showing changes in the levels of phospho-GSK-3α Ser^{21} and phospho-GSK-3β Ser^{9} normalized to their respective GSK-3 isoform protein levels. *D*, quantitative results showing changes in the levels of phospho-GSK-3α Tyr^{279} and phospho-GSK-3β Tyr^{216} normalized to their respective isoform protein levels. The results in *B–D* are expressed as the means ± S.E. of protein levels from three independent cultures. *, $p < 0.05$ compared with the respective control; **, $p < 0.01$; ***, $p < 0.001$. *E*, immunostaining of phospho-GSK-3β Ser^{9} in cortical neurons transfected with GSK-3α siRNA (*siGSK-3α*; P1375). Shown are immunocytochemical staining and confocal images of phospho-GSK-3β Ser^{9} in cortical neurons transfected with GSK-3α siRNA (P1375) or non-targeting control siRNA at 9 DIV for 48 h. Fluorescein isothiocyanate (*green*)-conjugated phospho-GSK-3β Ser^{9} staining indicates cytoplasmic and nuclear staining of phospho-GSK-3β Ser^{9} in non-targeting control siRNA- and GSK-3α siRNA-treated cortical neurons, respectively. Cultures were also stained with DAPI to detect nuclei (*blue*), and merged images (fluorescein isothiocyanate-conjugated phospho-GSK-3β Ser^{9}/DAPI) are shown for comparison. Confocal images were obtained by Zeiss LSM 510 microscopy using a digital camera 48 h after transfection. Representative images are shown. *Scale bars* = 50 μm.

overall GSK-3 kinase activity, as evidenced by an increase in β-catenin levels, similar to GSK-3 inhibition caused by treatment with small molecule inhibitors (3, 24). The cross-talk and autoregulation between two GSK-3 isoforms may thus account for these surprising and robust neuroprotective effects following GSK-3 isoform protein depletion in the neuronal systems that we examined. To better understand the status of GSK-3 serine and tyrosine phosphorylation in response to kinase inhibition, the effects of GSK-3 inhibitors on the phosphorylation levels of both GSK-3α and GSK-3β were also investigated in cortical neurons. As expected, treatment of these neurons with either GSK-3β inhibitor I (5 μM) or inhibitor VII (1 μM) for 24 h increased the phosphorylation levels of GSK-3α Ser^{21} (Fig. 5*A*), yet the relative GSK-3β Ser^{9} phosphorylation levels to total GSK-3β levels were unaffected by either inhibitor I or VII at the concentration used. An increase in Ser^{9} phosphorylation of GSK-3β was observed only at a higher concentration (5 μM) of inhibitor VII (data not shown). Conversely, the relative phosphorylation levels of GSK-3α Tyr^{279} and GSK-3β Tyr^{216} were decreased by inhibitors I and VII after 24 h of treatment. Interestingly, treatment with 1 mM LiCl for 24 h increased the phosphorylation levels of GSK-3α Ser^{21} and GSK-3β Ser^{9}, with no significant effects on the relative phosphorylation levels of GSK-3α Tyr^{279} and GSK-3β Tyr^{216} (Fig. 5*B*). A decrease in the level of GSK-3β Tyr^{216} phosphorylation was observed only at a higher concentration (2 mM) of lithium (data not shown). These results suggest that GSK-3 small molecule inhibitors and lithium have distinct effects on GSK-3 serine and tyrosine phosphorylation levels and that autoregulation of tyrosine phosphorylation of both GSK-3 isoforms could occur in response to GSK-3 inhibition. Consistent with results obtained from isoform gene silencing, our data demonstrated that increased Ser^{21} phosphorylation of

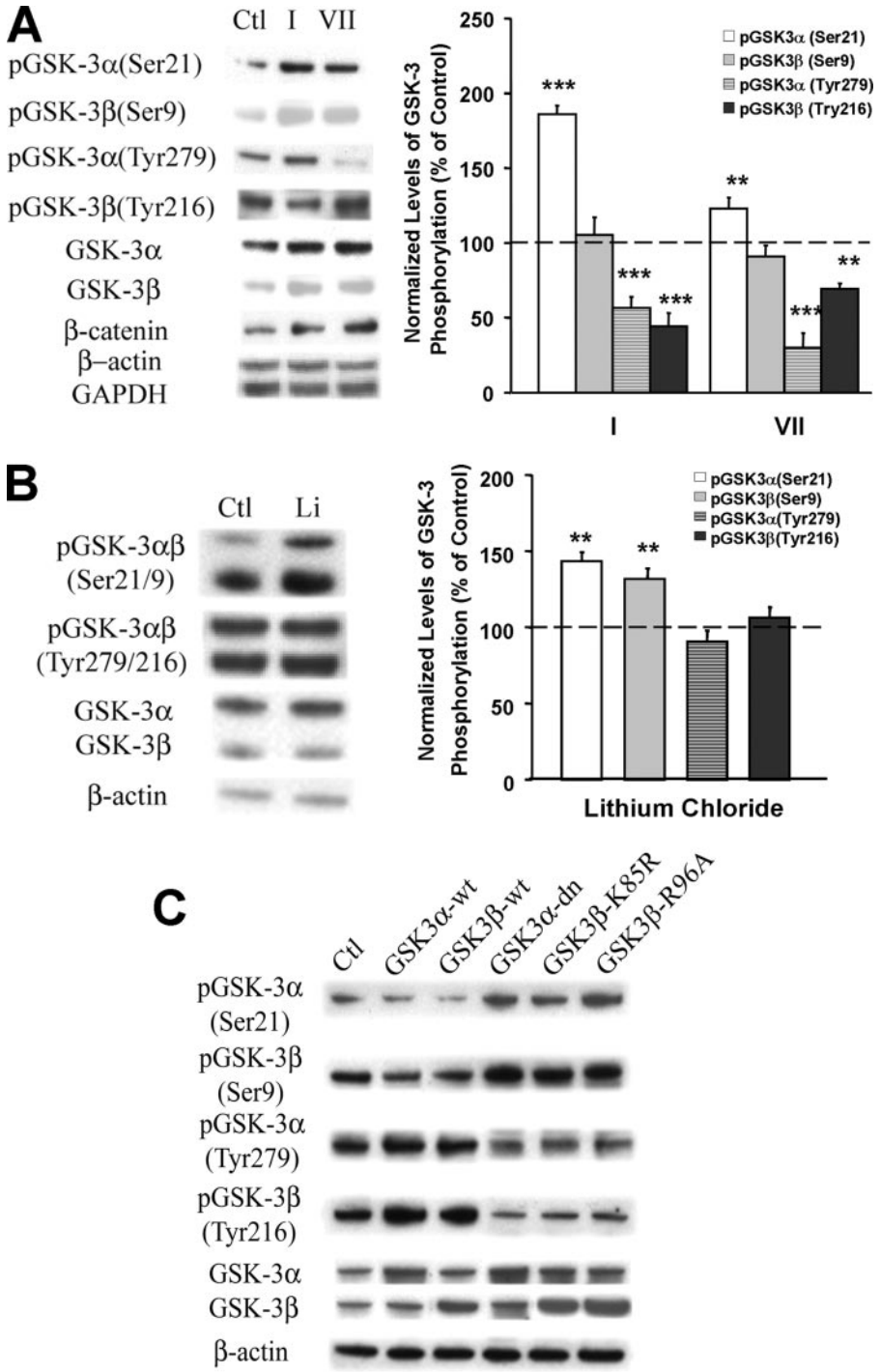

FIGURE 5. **Phosphorylation of GSK-3α Ser^{21}/GSK-3β Ser^{9} and dephosphorylation of GSK-3α Tyr^{279}/GSK-3β Tyr^{216} induced by GSK-3 inhibition.** *A*, representative Western blots and quantified results of GSK-3 isoforms and their phosphorylation levels in cortical neurons treated with GSK-3 inhibitor I (5 μM) or VII (1 μM) for 24 h. *Ctl*, control; *pGSK-3*, phospho-GSK-3. *B*, representative Western blots and quantified results of GSK-3 isoforms and their phosphorylation levels in cortical neurons treated with lithium chloride (*Li*; 1 mM) for 24 h. β-Actin and GAPDH were used as loading controls. The data are shown as the means ± S.E. of the relative levels of phosphorylation normalized to the respective isoform protein from three independent cultures. **, $p < 0.01$ compared with the respective control; ***, $p < 0.001$. *C*, representative Western blots of GSK-3 isoforms and their serine and tyrosine phosphorylation levels in cortical neurons transfected with wild-type (*wt*) GSK-3 isoforms or their dominant-negative (*dn*) mutants. Transfection was performed at the day of plating, and cultures were continued for 11 DIV. β-Actin was used as a loading control.

GSK-3α and reduced tyrosine phosphorylation of both isoforms resulted in enhanced β-catenin protein levels in cortical neurons treated with inhibitors I and VII (Fig. 5*A*), further indicating inhibition of GSK-3 activity. Increased Ser$^{21/9}$ phosphorylation and decreased Tyr$^{279/216}$ phosphorylation were observed in neurons transfected with dominant-negative mutant forms of GSK-3α and GSK-3β (Fig. 5*C*), whereas overexpression of wild-type GSK-3α or GSK-3β caused a decrease in the Ser^{21} and Ser^{9} phosphorylation levels of GSK-3α and GSK-3β, respectively. These results further support the notion that an increase in N-terminal serine phosphorylation and the resulting inhibition of GSK-3 kinase activity contribute to the neuroprotective effects of GSK-3 inhibition against glutamate-induced apoptosis.

GSK-3 Inhibitors Induce an Early Onset of Increased GSK-3α Ser^{21} Phosphorylation Levels but a Delayed Increase in GSK-3β Ser^{9} Phosphorylation—An increase in GSK-3β Ser^{9} phosphorylation in Neuro2A cells treated with GSK-3β small molecule inhibitor I for 24 h at a higher concentration (24) was not observed under our experimental conditions (Fig. 5*A*). We thus further examined the effects of GSK-3 inhibitors I and VII on GSK-3 serine phosphorylation in a time course experiment. An increase in GSK-3α Ser^{21} phosphorylation levels normalized to total GSK-3α protein levels was found as early as 4 h post-treatment and was maintained at an elevated level throughout the 4-day period of investigation (Fig. 6, *A* and *B*). On the other hand, an increase in normalized GSK-3β Ser^{9} phosphorylation did not occur until 4 days post-treatment using these two inhibitors under similar treatment conditions (Fig. 6, *A* and *C*). These results are also supported by a separate experiment using a GSK-3β fast activated cell-based enzyme-linked immunosorbent assay (FACE^{TM}) kit with modifications (supplemental Fig. S1*C*). Thus, up-regulation of serine phosphorylation of GSK-3α in response to treatment with these inhibitors was much more rapid than that of GSK-3β. Moreover, cortical neurons treated with either GSK-3 inhibitor showed reduced tyrosine phosphorylation of both GSK-3α and GSK-3β at 1 and 4 days, but not 4 h

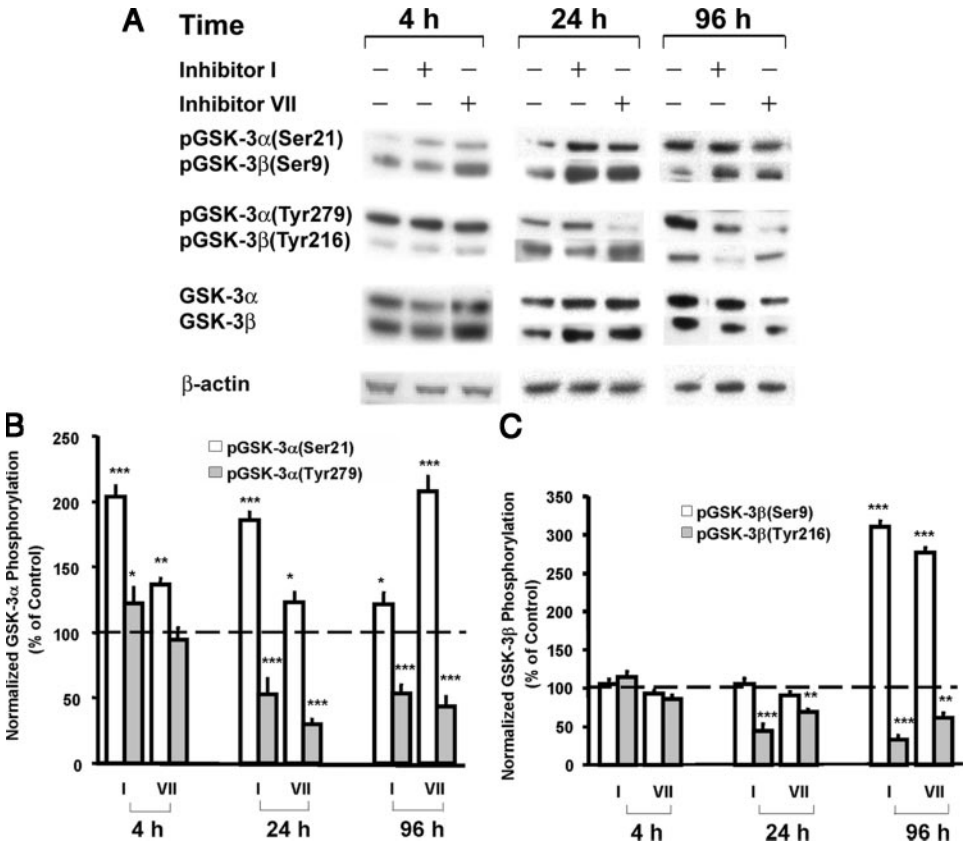

FIGURE 6. **Differential time requirement for the change in serine phosphorylation of GSK-3α and GSK-3β in response to treatment with GSK-3 inhibitors.** Cortical neurons at different stages were treated with inhibitor I (5 μM) or inhibitor VII (1 μM) for 4, 24, or 96 h. All cultures were harvested at 11 DIV for Western blot analysis. *A*, representative Western blots of phospho-GSK-3α Ser^{21}, phospho-GSK-3β Ser^{9}, phospho-GSK-3α Tyr^{279}, phospho-GSK-3β Tyr^{216}, GSK-3α, and GSK-3β. β-Actin was used as a loading control. *pGSK-3*, phospho-GSK-3. *B*, quantified results showing serine and tyrosine phosphorylation of GSK-3α. *C*, quantified results showing serine and tyrosine phosphorylation of GSK-3β. The data are expressed as the means ± S.E. of phosphorylation levels normalized to their respective isoform protein from three independent cultures. *, $p < 0.05$ compared with the 100% control; **, $p < 0.01$; ***, $p < 0.001$.

after treatment (Fig. 6, *A–C*). Treatment of cortical neurons with LiCl (2 mM) for 4 h increased the phosphorylation level of GSK-3α Ser^{21}, but not GSK-3β Ser^{9} (data not shown), again supporting the observation that serine phosphorylation of GSK-3α is more rapidly up-regulated compared with that of GSK-3β following GSK-3 inhibition. It is worth noting that treatment with GSK-3 inhibitors caused time-dependent biphasic changes in total GSK-3α and GSK-3β protein levels (Fig. 6*A*). This observation was also supported by measurement of GSK-3β protein levels using enzyme-linked immunosorbent assay, as both inhibitors caused an initial increase followed by a decrease in total GSK-3β protein levels in cortical neurons (supplemental Fig. S1*B*).

Decreased GSK-3β Ser^{9} Phosphorylation during Cortical Neuronal Maturation and Rescue of Spontaneous Cell Death by GSK-3 Gene Silencing—Our data thus far suggest that neuronal survival induced by GSK-3 depletion may be mediated in part through increased serine phosphorylation and decreased tyrosine phosphorylation and, more important, a possible cross-talk between the two isoforms of GSK-3 that manifests in a form of autophosphorylation (24). GSK-3 acts as an inhibitory component of Wnt signaling during embryonic development and cell proliferation in adult tissues (4). Regulation of Wnt/GSK-3 signaling has been implicated in neuronal development, maturation/differentiation, and aging of the mammalian central neuronal system (44–46). More important, disruption of the murine GSK-3β gene results in embryonic lethality presumably due to the activation of NF-κB, and the remaining GSK-3α cannot compensate for the functions of GSK-3β (33).

We therefore examined whether the expression and phosphorylation levels of GSK-3 isoforms and several GSK-3 kinase activity-associated proteins were altered during the course of maturation/aging of rat cortical neurons in cultures. The proteins examined included phospho-AKT Ser^{476}, phospho-ERK (p44/42), phospho-CREB Ser^{133}, β-catenin, and CDK5 because it has been reported that increased levels of phosphorylated AKT (phospho-AKT Ser^{476}) and ERK (phospho-ERK p44/42) cause enhanced serine phosphorylation of GSK-3 and thus inhibit GSK-3β activity (11). In addition, GSK-3 is known to phosphorylate both β-catenin and CREB and to regulate degradation of free β-catenin and the phosphorylation levels of CREB Ser^{133} (3). Moreover, CDK5 is a multifaceted kinase implicated in both the development and disease of the mammalian central nervous system (47). Total proteins for GSK-3, CREB, AKT, and ERK were examined for comparison. We found that there was a slight (~20%) decrease in the protein levels of GSK-3α and GSK-3β from 4 to 12 DIV, whereas the levels of phospho-AKT, CDK5, β-actin, and GAPDH were unchanged (Fig. 7*A*). Remarkably, there was a robust decrease in the phosphorylation levels of GSK-3β Ser^{9}. Normalization of phosphorylated GSK-3 isoforms to respective total GSK-3 protein revealed that phospho-GSK-3β Ser^{9} was decreased in a time-dependent manner, with an almost 80% loss at 12 DIV (Fig. 7*B*). In contrast, the normalized levels of phospho-GSK-3α Ser^{21}, phospho-GSK-3α Tyr^{279}, and phospho-GSK-3β Tyr^{216} were essentially unchanged. The β-catenin protein levels were attenuated with time in cultures with an ~50% decrease from 6 to 12 DIV (Fig. 7, *A* and *C*). These results again confirm our notion that the serine and tyrosine phosphorylation of the two GSK-3 isoforms are differentially regulated. The levels of CREB protein were changed biphasically; they were slightly increased from 4 to 8 DIV, followed by a decline (Fig. 7, *A* and *C*), yet a progressive decrease in the phosphorylation levels of CREB Ser^{133} was observed. The decreases in the levels of phospho-CREB Ser^{133} and total β-catenin protein are indicative of increased GSK-3 activity. In contrast, the levels of

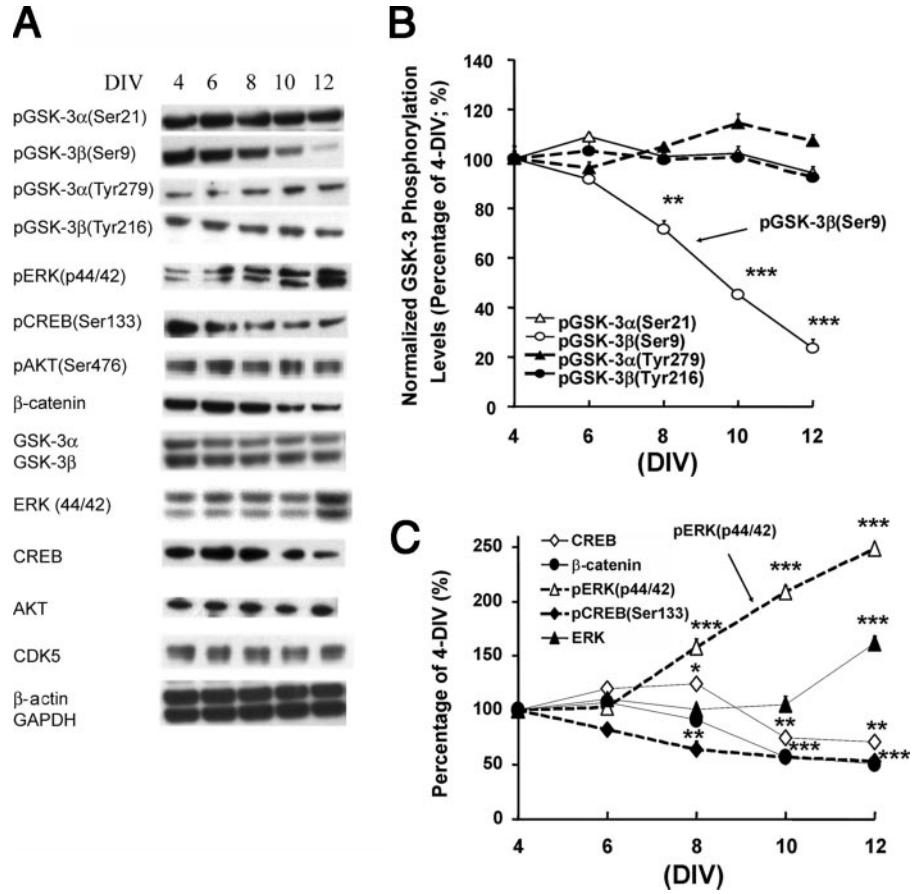

FIGURE 7. **Phosphorylation states of GSK-3α and GSK-3β and GSK-3 kinase activity at various stages of cortical neuronal culture.** Cortical neurons were cultured for the indicated DIV and then harvested for Western blot analysis. *A*, representative Western blots of the levels of phospho-GSK-3α Ser^{21}, phospho-GSK-3β Ser^{9}, phospho-GSK-3α Tyr^{279}, phospho-GSK-3β Tyr^{216}, phospho-ERK (p44/42), phospho-CREB Ser^{133}, phospho-AKT Ser^{476}, β-catenin, GSK-3α, GSK-3β, ERK (p44/42), CREB, AKT, and CDK5. β-Actin and GAPDH were used as loading controls. *pGSK-3*, phospho-GSK-3. *B*, quantified results showing progressive and robust reduction in the normalized phospho-GSK-3β Ser ^{9} levels, but a slight steady increase in the normalized GSK-3α serine and tyrosine phosphorylation levels. *C*, quantified results showing reduced levels of phospho-CREB Ser^{133}, CREB, and β-catenin in neurons, but a marked increase in the levels of ERK and phospho-ERK (p44/42) in culture. The data are expressed as the means ± S.E. of the percentage of the control at 4 DIV from three independent cultures. *, $p < 0.05$; **, $p < 0.01$; ***, $p < 0.001$.

phospho-ERK Thr^{202}/Tyr^{204} (phospho-p44/42 MAPK) were robustly increased with time in cultures, with an ~250% increase from 6 to 12 DIV.

Because cortical neurons undergo spontaneous cell death in culture, the progressive reduction in phospho-GSK-3β Ser^{9} levels indicative of increased GSK-3 activity might contribute to this form of cell death. We thus investigated the effects of GSK-3 depletion by RNA interference in cortical neurons undergoing maturation for up to 12 DIV. Efficient protein depletion of either GSK-3α and GSK-3β resulted in a respective increase in normalized Ser$^{21/9}$ phosphorylation of GSK-3α/β throughout the time course we examined (Fig. 8, *A* and *B*), similar to the results described above (Fig. 4, *A*–*C*). Thus, GSK-3 RNA interference abolished the maturation-induced decrease in normalized GSK-3β Ser^{9} phosphorylation (Fig. 8, *A* and *B*). In addition, GSK-3 isoform depletion blocked the maturation-induced loss of β-catenin (Fig. 8*A*).

We next investigated the effects of RNA interference-mediated GSK-3 depletion on spontaneous neuronal death in an extended cortical culture. Under our culture conditions, viability progressively decreased, with an ~20% reduction at 12 DIV and a >80% decrease at 36 DIV compared with the 8 DIV control (Fig. 9*A*). To assess the role of GSK-3α and GSK-3β neuronal death in the extended culture, siRNA specific for GSK-3α or GSK-3β was transfected into cortical neurons at the time of plating, followed by another transfection at 14 DIV to ensure effective GSK-3 gene silencing throughout the course of the extended neuronal culture. Selective gene silencing effects were confirmed by Western blot analysis at 8, 12, 16, 26, and 36 DIV (data not shown). Cell viability determined by MTT assay at 12, 16, 26, and 36 DIV was significantly enhanced by transfection with siRNA for GSK-3α or GSK-3β (Fig. 9*B*). Interestingly, GSK-3β protein depletion was more effective than GSK-3α depletion in promoting neuronal survival throughout the course of the culture extension up to 36 DIV days, thus supporting our hypothesis that decreased serine phosphorylation of GSK-3β may contribute to spontaneous neuronal death. These results are compatible with our previous suggestion that increased serine phosphorylation induced by GSK-3 protein depletion may contribute to neuronal survival against glutamate insult. Similar differential protective effects of GSK-3 gene silencing on cell survival were obtained using a lactate dehydrogenase assay in cortical neurons cultured for an extended period (Fig. 9*C*). These different extents of neuroprotective effects resulting from protein depletion of GSK-3 isoforms were also observed at 16 and 26 DIV in an independent 96-well viability assay using double fluorescence staining of calcein-AM and EthD-1 for the detection of live and dead cells, respectively (Fig. 9*D*). Fig. 9*E* shows the effective staining of untreated neurons at 8 DIV with calcein-AM and EthD-1 by confocal and Z-sectioning imaging. Staining with calcein-AM/EthD-1 in extended cortical cultures at 26 DIV confirmed the neuroprotective effects of GSK-3β siRNA (supplemental Fig. S2).

DISCUSSION

In this study, we employed GSK-3 isoform-specific siRNAs, dominant-negative mutants, and small molecule inhibitors to assess the similarities and differences in the function and regulation of GSK-3α and GSK-3β. We found that inhibition of

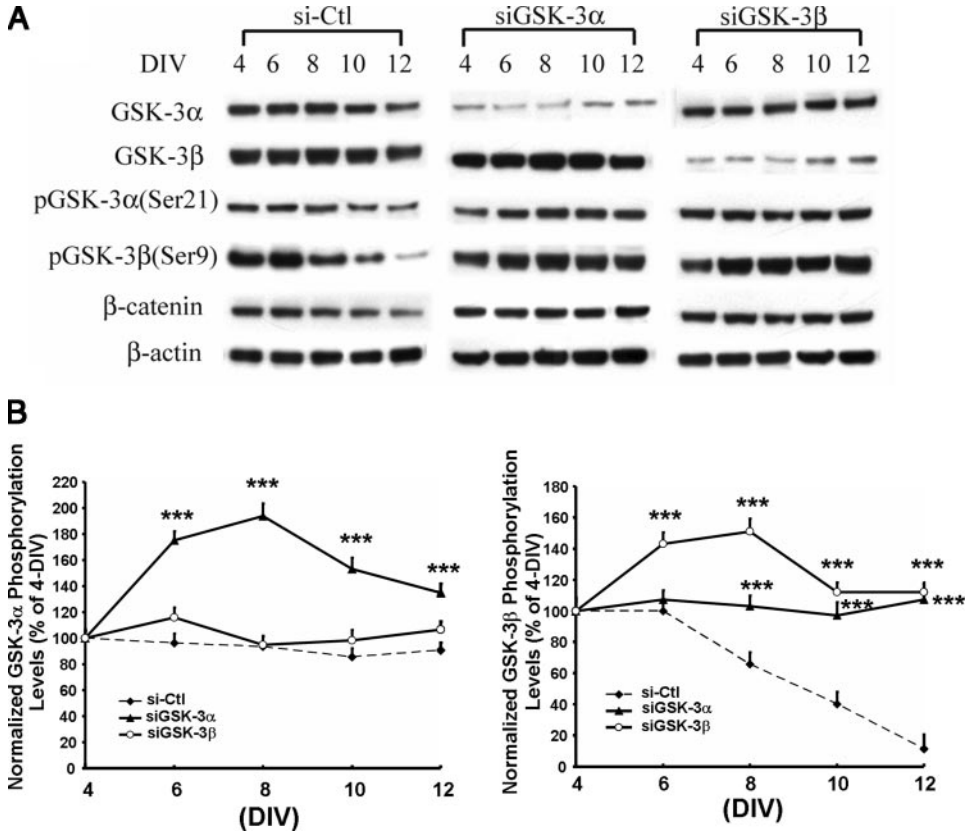

FIGURE 8. **Autoregulation of phospho-GSK-3α Ser^{21}/phospho-GSK-3β Ser^{9} induced by GSK-3 isoform-specific siRNA during neuronal maturation.** *A*, representative Western blot analysis of the levels of phospho-GSK-3α Ser^{21}, phospho-GSK-3β Ser^{9}, GSK-3α, GSK-3β, and β-catenin at the indicated DIV. Cortical neurons were transfected with isoform-specific siRNA mixtures at the time of plating. Cell lysates from different DIV were collected for Western blot analysis. β-Actin was used as a loading control. *si-Ctl*, non-targeting control siRNA; *siGSK-3*, GSK-3 siRNA; *pGSK-3*, phospho-GSK-3. *B*, quantitative results showing changes in the levels of phospho-GSK-3α Ser^{21} and phospho-GSK-3β Ser^{9} normalized to their respective GSK-3 isoform protein levels. The data are expressed as the means $\pm$ S.E. of protein levels from three independent cultures. ***, $p < 0.001$ compared with the control siRNA at the respective DIV.

GSK-3 by reduction in GSK-3 isoform protein expression, treatment with lithium and other GSK-3 small molecule inhibitors, or overexpression of dominant-negative mutants leads to protection against glutamate insult in cultured cortical neurons. Interestingly, we found that siRNA-mediated depletion of one GSK-3 isoform or overexpression of GSK-3 isoform-specific dominant-negative mutants is sufficient to achieve essentially complete suppression of glutamate excitotoxicity. This unexpected observation may be explained in part by the cross-talk between GSK-3 isoforms. Our results show that gene silencing of either GSK-3α or GSK-3β causes a reduction in Tyr^{216} phosphorylation of GSK-3β and an increase in the serine phosphorylation levels (and thus enhanced enzymatic inhibition) of the remaining isoforms. GSK-3 kinase inactivation by autophosphorylation is likely part of the molecular mechanisms underlying neuroprotection. GSK-3β Ser^{9} phosphorylation does not seem to contribute to inhibition of GSK-3β in response to Wnt proteins (48, 49); however, accumulation of β-catenin induced by GSK-3α and GSK-3β depletion and pharmacological inhibition under our conditions suggests the inhibition of GSK-3 activity.

This study has further documented that GSK-3β protein depletion modestly decreased the tyrosine phosphorylation levels of both isoforms, whereas GSK-3α depletion markedly increased the phosphorylation levels of GSK-3α Tyr^{279} but decreased those of GSK-3β Tyr^{216}. Moreover, tyrosine phosphorylation of GSK-3α and GSK-3β in cortical neurons was decreased after treatment with either GSK-3β inhibitor I or VII for 1 day or longer. Our data are supported by a previous study demonstrating that GSK-3β is capable of catalyzing the autophosphorylation of Tyr^{216} *in vitro* (26) and suggest that the phosphorylation of Tyr$^{279/216}$ in cells is also catalyzed by GSK-3. However, our results are in variance with other previous reports that GSK-3β Tyr^{216} phosphorylation is not autoregulated following GSK-3 inhibition (21, 25). Together, these results suggest a vast complexity and isoform specificity in the regulation of tyrosine phosphorylation of GSK-3 isoforms in response to their silencing or inhibition. A time course experiment using GSK-3 inhibitors I and VII showed early onset of the up-regulation of GSK-3α serine phosphorylation compared with changes in GSK-3β serine phosphorylation and GSK-3 tyrosine phosphorylation, suggesting that distinct mechanisms are involved in the regulation of serine and tyrosine phosphorylation of GSK-3α and GSK-3β. We are currently investigating whether the enhanced GSK-3α Ser^{21} phosphorylation serves as a primer to trigger drug-induced regulation of GSK-3β Ser^{9} and GSK-3α and GSK-3β tyrosine phosphorylation possibly via autophosphorylation.

Surprisingly, treatment of neurons with either of the two non-ATP-competitive GSK-3 inhibitors (inhibitors I and VII) caused a fluctuation in the total GSK-3 protein levels under our conditions by yet unidentified mechanisms. A decrease in total GSK-3 protein levels was also observed in cortical neurons treated with two ATP-competitive GSK-3 inhibitors (SB 216763 and SB 415286) for 48 h (supplemental Fig. S3). GSK-3β is distributed into several distinct subcellular pools such as the cytosol, nucleus, and mitochondria. Subcellular allocation of GSK-3β likely contributes to its functional regulation (7). An assessment of the subcellular distribution of total and phosphorylated GSK-3 isoforms in neurons treated with various GSK-3 inhibitors is thus desirable to elucidate the underlying mechanisms and biological consequences in neurons following treatment with small molecule inhibitors. In addition, it has been reported that SB 216763 and SB 415286 cause a decrease in the phosphorylation levels of GSK-3β Ser^{9}, an effect possibly medi-

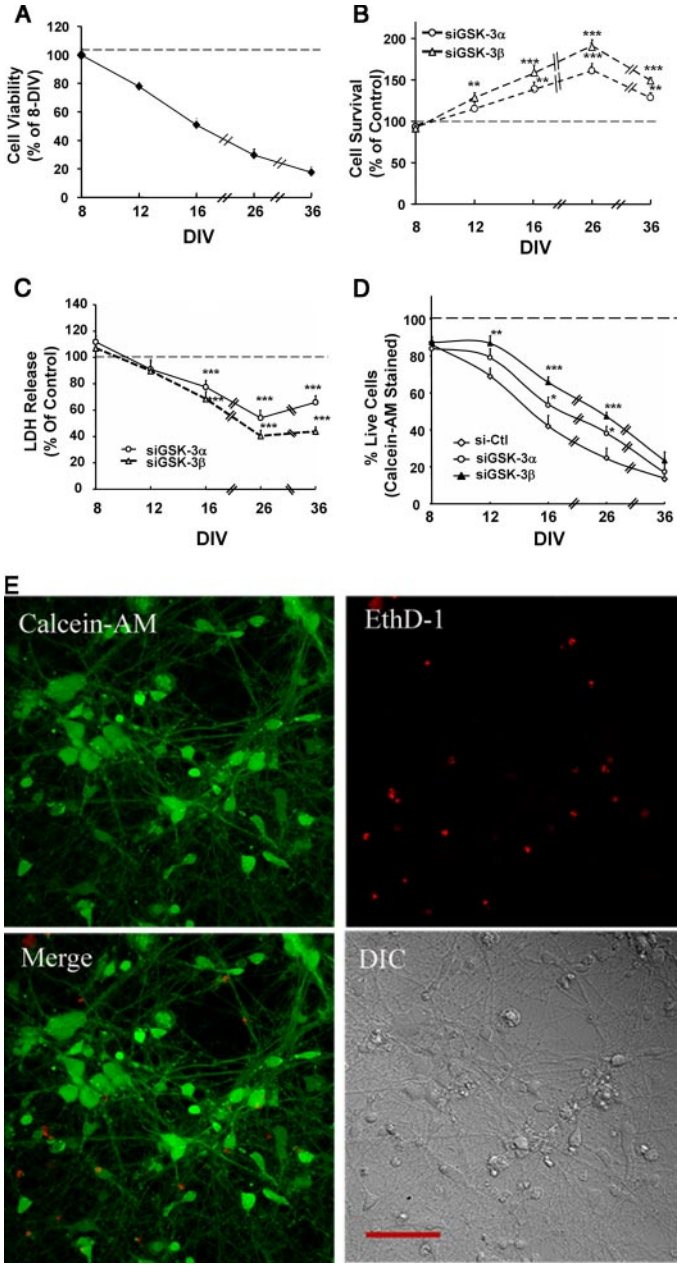

FIGURE 9. **Neuroprotective effects of isoform-specific siRNAs on spontaneous neuronal death in extended culture.** *A*, cortical cultures were harvested at the indicated DIV for the determination of cell viability by MTT assay. The data are shown as the means ± S.E. of the percentage of the control at 8 DIV from six independent cultures. *B*, cortical neurons were transfected with 80 nM rat GSK-3α- or GSK-3β-specific siRNA mixture or non-targeting control siRNA using a Nucleofector device at the time of plating as described under "Materials and Methods." At 14 DIV, cultures were again transfected with the above-described siRNA using 80 nM siPORT *Amine* transfection reagent. Cells were harvested at the indicated DIV for viability determination by MTT assay. The data are shown as the means ± S.E. of the percentage of the respective non-targeting control siRNA from six independent cultures. *siGSK-3*, GSK-3 siRNA. **, $p < 0.01$; ***, $p < 0.001$. *C*, cortical cultures were transfected exactly as described for *B* and harvested at the indicated DIV for the determination of cell viability by lactate dehydrogenase (*LDH*) assay. The data are shown as the means ± S.E. of the percentage of the respective non-targeting control siRNA from four independent cultures. ***, $p < 0.001$ *D*, cortical neurons were cultured in 96-well plates, transfected exactly as described for *B*, and harvested at the indicated DIV for the determination of cell viability by live/dead viability/cytotoxicity analysis, which provides a two-color fluorescence to determine live and dead cells simultaneously using a fluorescence microplate reader. Calcein-AM (3 μM) and EthD-1 (1 μM) were the dyes used in this application. The percentage of calcein-AM-labeled live cells was determined according to the manufacturer's recommendation. The data are shown as the means ± S.E. of the percentage of the respective non-targeting control siRNA (*si-Ctl*) from four independent cultures. *, $p < 0.05$; **, $p < 0.01$; ***, $p < 0.001$. *E*, shown are the results from confocal imaging of live and dead cells determined at 8 DIV. Cultures were transfected with GSK-3β siRNA as described above and incubated at 8 DIV with 6 μM calcein-AM and 2 μM EthD-1 at room temperature for 45 min. Green fluorescence (calcein-AM)-labeled live cells and red fluorescence (EthD-1)-labeled dead cells were examined by laser scanning confocal microscopy (Zeiss LSM 510 413), and Z-sectioning images were captured using a digital camera. Also shown are their merged and Nomarski-DIC images. Representative images are shown. *Scale bar* = 50 μm.

ated through their inhibition on p90^{rsk2}, which directly phosphorylates GSK-3β Ser^{9} (24, 50). We also examined the effects of these two inhibitors in cultured cortical neurons and found similar results of reduced serine phosphorylation (supplemental Fig. S3). The development of more potent and selective GSK-3 inhibitors should result in a better understanding of the complex functions of GSK-3.

The roles for GSK-3 in neuronal differentiation, maturation, and development are well recognized. For example, overexpression of GSK-3β in the central nervous system of developing mice results in a reduction in the size of the brain and spinal cord (46), and GSK-3β gene disruption causes embryonic lethality (33). During the aging of human fibroblasts, the active form of GSK-3β accumulates in the nucleus in association with p53, causing replicative senescence (51). Our approaches using two-step gene silencing and Western blotting in extended cultures confirmed the efficient depletion of specific isoforms as well as enhanced N-terminal serine phosphorylation, indicative of reduced GSK-3 kinase activity throughout the period examined (data not shown). Although GSK-3β protein depletion was more effective than GSK-3α protein depletion in improving neuronal survival in the extended culture, the disruption of either GSK-3 isoform was capable of increasing the survival of neurons, likely due to autophosphorylation induced by cross-talk between the two isoforms. Tightly regulated serine phosphorylation of GSK-3 in maturing neurons thus likely controls multiple endogenous downstream signaling pathways, including aging-induced apoptosis.

Of interest, the down-regulation of GSK-3β Ser^{9} was inversely correlated with an up-regulation of phospho-ERK (p44/42) in extended cultures. This result is consistent with a recent report that GSK-3 acts as an endogenous negative regulator of ERK1/2 through protein kinase Cδ (52). Additionally, ERK1/2 is known to inhibit GSK-3 via the Ras/ERK/ribosomal S6 kinase/GSK-3 signaling cascade (reviewed in Ref. 16). It thus seems possible that GSK-3β activation in conjunction with ERK activation is involved in the differentiation and/or maturation of cortical neurons in cultures. On the other hand, phospho-ERK (p44/42) was found to be up-regulated in striatal cells expressing mutant huntingtin, leading to cell death (53). It is conceivable that activation of GSK-3β resulting from its loss of serine phosphorylation is an initial signal triggering a program that ultimately executes neuronal death in extended cultures. The latter possibility is in line with our results that the levels of cytoprotective phospho-CREB Ser^{133} and total CREB protein are decreased with time in culture and the observation that overexpression of GSK-3β blocks CREB DNA-binding activity induced by growth factors (54).

The precise mechanisms underlying the differential phosphorylation and dephosphorylation of GSK-3α and GSK-3β observed in this study remain to be defined. It has been suggested that Tyr^{216} phosphorylation of GSK-3β may be regulated by the Src-like Fyn kinase, Ca^{2+}-sensitive PYK2 (proline-rich tyrosine kinase-2), a putative homolog of *Dictyostelium* ZAK1 (zaphod kinase-1) tyrosine kinase, and MEK1 (MAPK/extracellular signal-regulated kinase kinase-1) (55). It has also been reported that serine phosphorylation of GSK-3 is mediated by protein kinases, including AKT, protein kinase A, protein kinase C, ERK1/2/$p90^{RSK}$, $p70^{S6K}$, and integrin-linked kinase (2–4), whereas protein phosphatases, including PP1 and PP2A, have been implicated in GSK-3 serine dephosphorylation (24, 56, 57). The autophosphorylation of GSK-3β Ser^9 elicited by GSK-3 inhibition or gene silencing is proposed to be due to the inhibition of PP1 activity and a positive feedback loop between GSK-3β and PP1 (24, 58). Thus, a reduction in GSK-3 activity results in a decrease in Thr^{72} phosphorylation of PP1 inhibitor-2 (and hence, activation of its inhibitory effect), causing suppression of PP1 activity and induction of GSK-3/PP1 inhibitor-2/PP1/GSK-3 autoregulatory circuitry. PP1 has critical roles in neuronal functions, including regulation of neurite formation (59) and modulation of glutamatergic neurotransmission (60) through binding to the scaffold protein neurabin I at different subcellular locations in maturing mammalian neurons (61, 62). It is noteworthy that GSK-3 and its inhibition have also been implicated in axonal morphology and synaptic protein clustering in developing neurons (63). In addition, GSK-3α and GSK-3β differ in their subcellular localizations (36, 54) and thus might be differentially regulated by interacting with distinct protein complexes such as PP1-neurabin I within subcellular organelles in response to treatment and during neuronal maturation/aging (37–39). Collectively, these reports underscore the complexity of the regulation of GSK-3 activity in neurons at different maturational stages or undergoing aging-induced apoptosis. The observed variations in the phosphorylation levels of GSK-3α and GSK-3β thus likely reflect the net effects of actions of protein kinases, protein phosphatases, and/or their subcellular localizations.

In conclusion, our study has demonstrated the similar and dissimilar regulation and function of GSK-3α and GSK-3β isoforms following either GSK-3 pharmacological inhibition/gene silencing or exposure to glutamate insult/neuronal aging in cortical cultures. Inhibition of either isoform alone is sufficient to protect neurons from glutamate insult, and the mechanisms could partly lie in the cross-talk between these two isoforms. Our results also demonstrate that, in response to inhibitor treatment, serine phosphorylation of these isoforms is temporally dissociated. A similar phenomenon is also observed in neurons undergoing maturation, where GSK-3β serine phosphorylation is selectively down-regulated. Given that aberrant GSK-3 activity has been implicated in the pathophysiology of neurological and neuropsychiatric disorders, the development of isoform-specific inhibitors or gene silencing seems to be essential for therapeutic intervention and a better understanding of the pathogenesis of these diseases.

Acknowledgments—We are grateful to Dr. Carolyn Smith (Neuroscience Light Imaging Facility, Division of Intramural Research, NINDS, National Institutes of Health) for superb assistance in confocal microscopy imaging. We thank Charlotte Wiest and Connie Chen for technical assistance, Dr. Yun Wang (Laboratory of Molecular Pathophysiology, National Institute of Mental Health) for valuable advice in confocal microscopy imaging, and Drs. Michael Rowe and Peter Leeds (Molecular Neurobiology Section, National Institute of Mental Health) for critical reading of this manuscript. The superb editorial assistance of the National Institutes of Health Fellows Editorial Board is also greatly appreciated.

REFERENCES

1. Woodgett, J. R. (1990) *EMBO J.* **9,** 2431–2438
2. Frame, S., and Cohen, P. (2001) *Biochem. J.* **359,** 1–16
3. Grimes, C. A., and Jope, R. S. (2001) *Prog. Neurobiol.* (*Oxf.*) **65,** 391–426
4. Doble, B. W., and Woodgett, J. R. (2003) *J. Cell Sci.* **116,** 1175–1186
5. Emamian, E. S., Hall, D., Birnbaum, M. J., Karayiorgou, M., and Gogos, J. A. (2004) *Nat. Genet.* **36,** 131–137
6. O'Brien, W. T., Harper, A. D., Jove, F., Woodgett, J. R., Maretto, S., Piccolo, S., and Klein, P. S. (2004) *J. Neurosci.* **24,** 6791–6798
7. Bijur, G. N., and Jope, R. S. (2003) *Neuroreport* **14,** 2415–2419
8. Iwahana, E., Akiyama, M., Miyakawa, K., Uchida, A., Kasahara, J., Fukunaga, K., Hamada, T., and Shibata, S. (2004) *Eur. J. Neurosci.* **19,** 2281–2287
9. Iitaka, C., Miyazaki, K., Akaike, T., and Ishida, N. (2005) *J. Biol. Chem.* **280,** 29397–29402
10. Yin, L., Wang, J., Klein, P. S., and Lazar, M. A. (2006) *Science* **311,** 1002–1005
11. Jope, R. S., and Johnson, G. V. (2004) *Trends Biochem. Sci.* **29,** 95–102
12. Klein, P. S., and Melton, D. A. (1996) *Proc. Natl. Acad. Sci. U. S. A.* **93,** 8455–8459
13. Stambolic, V., Ruel, L., and Woodgett, J. R. (1996) *Curr. Biol.* **6,** 1664–1668
14. Manji, H. K., Moore, G. J., and Chen, G. (1999) *Biol. Psychiatry* **46,** 929–940
15. Jope, R. S., and Bijur, G. N. (2002) *Mol. Psychiatry* **7,** Suppl. 1, S35–S45
16. Rowe, M. K., and Chuang, D.-M. (2004) *Expert Rev. Mol. Med.* **6,** 1–18
17. Takashima, A., Noguchi, K., Sato, K., Hoshino, T., and Imahori, K. (1993) *Proc. Natl. Acad. Sci. U. S. A.* **90,** 7789–7793
18. Pap, M., and Cooper, G.M. (1998) *J. Biol. Chem.* **273,** 19929–19932
19. Maggirwar, S. B., Tong, N., Ramirez, S., Gelbard, H. A., and Dewhurst, S. (1999) *J. Neurochem.* **73,** 578–586
20. Hetman, M., Cavanaugh, J. E., Kimelman, D., and Xia, Z. (2000) *J. Neurosci.* **20,** 2567–2574
21. Bhat, R. V., Shanley, J., Correll, M. P., Fieles, W. E., Keith, R. A., Scott, C. W., and Lee, C. M. (2000) *Proc. Natl. Acad. Sci. U. S. A.* **97,** 11074–11079
22. Bijur, G. N., De Sarno, P., and Jope, R. S. (2000) *J. Biol. Chem.* **275,** 7583–7590
23. Bijur, G. N., and Jope, R. S. (2001) *J. Biol. Chem.* **276,** 37436–37442
24. Zhang, F., Phiel, C. J., Spece, L., Gurvich, N., and Klein, P. S. (2003) *J. Biol. Chem.* **278,** 33067–33077
25. Wang, Q. M., Fiol, C. J., DePaoli-Roach, A. A., and Roach, P. J. (1994) *J. Biol. Chem.* **269,** 14566–14574
26. Cole, A., Frame, S., and Cohen, P. (2004) *Biochem. J.* **377,** 249–255
27. Hughes, K., Nikolakaki, E., Plyte, S. E., Totty, N. F., and Woodgett, J. R. (1993) *EMBO J.* **12,** 803–808
28. Kim, L., Liu, J., and Kimmel, A. R. (1999) *Cell* **99,** 399–408
29. Lesort, M., Jope, R. S., and Johnson, G. V. (1999) *J. Neurochem.* **72,** 576–584
30. Hartigan, J. A., Xiong, W. C., and Johnson, G. V. (2001) *Biochem. Biophys. Res. Commun.* **284,** 485–489
31. Goode, N., Hughes, K., Woodgett, J. R., and Parker, P. J. (1992) *J. Biol. Chem.* **267,** 16878–16882

32. Wang, Q. M., Park, I. K., Fiol, C. J., Roach, P. J., and DePaoli-Roach, A. A. (1994) *Biochemistry* **33,** 143–147
33. Hoeflich, K. P., Luo, J., Rubie, E. A., Tsao, M. S., Jin, O., and Woodgett, J. R. (2000) *Nature* **406,** 86–90
34. Phiel, C. J., Wilson, C. A., Lee, V. M., and Klein, P. S. (2003) *Nature* **423,** 435–439
35. Su, Y., Ryder, J., Li, B., Wu, X., Fox, N., Solenberg, P., Brune, K., Paul, S., Zhou, Y., Liu, F., and Ni, B. (2004) *Biochemistry* **43,** 6899–6908
36. Hoshi, M., Sato, M., Kondo, S., Takashima, A., Noguchi, K., Takahashi, M., Ishiguro, K., and Imahori, K. (1995) *J. Biochem.* (*Tokyo*) **118,** 683–685
37. Franca-Koh, J., Yeo, M., Fraser, E., Young, N., and Dale, T. C. (2002) *J. Biol. Chem.* **277,** 43844–43848
38. Watcharasit, P., Bijur, G. N., Zmijewski, J. W., Song, L., Zmijewska, A., Chen, X., Johnson, G. V., and Jope, R. S. (2002) *Proc. Natl. Acad. Sci. U. S. A.* **99,** 7951–7955
39. Watcharasit, P., Bijur, G. N., Song, L., Zhu, J., Chen, X., and Jope, R. S. (2003) *J. Biol. Chem.* **278,** 48872–48879
40. Hashimoto, R., Hough, C., Nakazawa, T., Yamamoto, T., and Chuang, D.-M. (2002) *J. Neurochem.* **80,** 589–597
41. Liang M.-H., and Chuang D.-M. (2006) *J. Biol. Chem.* **281,** 30479–30484
42. Chen, G., Bower, K. A., Ma, C., Fang, S., Thiele, C. J., and Luo, J. (2004) *FASEB J.* **18,** 1162–1164
43. Chalecka-Franaszek, E., and Chuang, D.-M. (1999) *Proc. Natl. Acad. Sci. U. S. A.* **96,** 8745–8750
44. Dominguez, I., Itoh, K., and Sokol, S. Y. (1995) *Proc. Natl. Acad. Sci. U. S. A.* **92,** 8498–8502
45. He, X., Saint-Jennet, J. P., Woodgett, J. R., Varmus, H., and Dawid, I. (1995) *Nature* **374,** 617–622
46. Spittaels, K., Van Den Haute, C., Van Dorpe, J., Terwel, D., Vandezande, K., Lasrado, R., Bruynseels, K., Irizarry, M., Verhoyle, M., Van Lint, J., Vandeenheede, J. R., Ashton, D., Mercken, M., Loos, R., Hyman, B., Van Der Linden, A., Geerts, H., and Van Leuven, F. (2002) *Neuroscience* **13,** 797–808
47. Cruz, J. C., and Tsai, L. H. (2004) *Curr. Opin. Neurobiol.* **14,** 390–394
48. Ruel, L., Stambolic, V., Ali, A., Manoukian, A. S., and Woodgett, J. R. (1999) *J. Biol. Chem.* **274,** 21790–21796
49. Ding, V. W., Chen, R. H., and McCormick, F. (2000) *J. Biol. Chem.* **275,** 32475–32481
50. Lochhead, P. A., Coghlan, M., Rice, S. Q., and Sutherland, C. (2001) *Diabetes* **50,** 937–946
51. Zmijewski, J. W., and Jope, R. S. (2004) *Aging Cell* **3,** 309–317
52. Wang, Q., Zhou, Y., Wang, X., and Evers, B. M. (2006) *Oncogene* **25,** 43–50
53. Apostol, B. L., Illes, K., Pallos, J., Bodai, L., Wu, J., Strand, A., Schweitzer, E., Olson, J. M., Kazantsev, A., Marsh, J. L., and Thompson, L. M. (2006) *Hum. Mol. Genet.* **15,** 273–285
54. Grimes, C. A., and Jope, R. S. (2001) *J. Neurochem.* **78,** 1219–1232
55. Meijer, L., Flajolet, M., and Greengard, P. (2004) *Trends Pharmacol. Sci.* **25,** 471–480
56. Welsh, G. I., and Proud, C. G. (1993) *Biochem. J.* **294,** 625–629
57. Sutherland, C., Leighton, I. A., and Cohen, P. (1993) *Biochem. J.* **296,** 15–19
58. Szatmari, E., Habas, A., Yang, P., Zheng, J. J., Hagg, T., and Hetman, M. (2005) *J. Biol. Chem.* **280,** 37526–37535
59. Nakanishi, H., Obaishi, H., Satoh, A., Wada, M., Mandai, K., Satoh, K., Nishioka, H., Matsuura, Y., Mizoguchi, A., and Takai, Y. (1997) *J. Cell Biol.* **139,** 951–961
60. Muly, E. C., Allen, P., Mazloom, M., Aranbayeva, Z., Greenfield, A. T., and Greengard, P. (2004) *Cereb. Cortex* **14,** 1398–1407
61. Oliver, C. J., Terry-Lorenzo, R. T., Elliott, E., Bloomer, W. A., Li, S., Brautigan, D. L., Colbran, R. J., and Shenolikar, S. (2002) *Mol. Cell. Biol.* **22,** 4690–4701
62. Terry-Lorenzo, R. T., Roadcap, D. W., Otsuka, T., Blanpied, T. A., Zamorano, P. L., Garner, C. C., Shenolikar, S., and Ehlers, M. D. (2005) *Mol. Biol. Cell* **16,** 2349–2362
63. Lucas, F. R., Goold, R. G., Gordon-Weeks, P. R., and Salinas, P. C. (1998) *J. Cell Sci.* **111,** 1351–1361